This is a post-print version of the manuscript published in Toxicology and Applied Pharmacology by Sindi et al., in October 2016

The full paper in journal format, together with accompanying supplementary materials, can be accessed via the following link:

http://dx.doi.org/10.1016/j.taap.2016.08.008

Chlorpyrifos- and chlorpyrifos oxon-induced neurite retraction in pre-differentiated N2a cells is associated with transient hyperphosphorylation of neurofilament heavy chain and ERK 1/2.

Ramya A. Sindi[1, 3], Wayne Harris[1], Gordon Arnott[2], John Flaskos[4], Chris Lloyd Mills[2], Alan J. Hargreaves[1]

[1]Interdisciplinary Biomedical Research Centre, School of Science and Technology, Nottingham Trent University, Clifton Lane, Nottingham, NG11 8NS, UK.

[2]School of Science and Technology, Nottingham Trent University, Nottingham, NG11 8NS, UK.

[3]School of Applied Medical Sciences, Umm Al-Qura University, Makkah, Saudi Arabia.

4Laboratory of Biochemistry and Toxicology, School of Veterinary Medicine, Aristotle University of Thessaloniki, 54124 Thessaloniki, Greece.

Corresponding authors:

E-mail: ramya.sindi2010@my.ntu.ac.uk (RAS)

alan.hargreaves@ntu.ac.uk (AJH)

Abstract

Chlorpyrifos (CPF) and CPF-oxon (CPO) are known to inhibit neurite outgrowth but little is known about their ability to induce neurite retraction in differentiating neuronal cells. The aims of this study were to determine the ability of these compounds to destabilize neurites and to identify the key molecular events involved. N2a cells were induced to differentiate for 20 h before exposure to CPF or CPO for 2-8 h. Fixed cell monolayers labeled with carboxyfluorescein succinimidyl ester or immunofluorescently stained with antibodies to tubulin (B512) or phosphorylated neurofilament heavy chain (Ta51) showed time- and concentration-dependent reductions in numbers and length of axon-like processes compared to the control, respectively, retraction of neurites being observed within 2 h of exposure by live cell imaging. Neurofilament disruption was also observed in treated cells stained by indirect immunofluorescence with anti-phosphorylated neurofilament heavy chain (NFH) monoclonal antibody SMI34, while the microtubule network was unaffected. Western blotting analysis revealed transiently increased levels of reactivity of Ta51 after 2 h exposure and reduced levels of reactivity of the same antibody following 8 h treatment with both compounds, whereas reactivity with antibodies to anti-total NFH or anti-tubulin was not affected. The alteration in NFH phosphorylation at 2 h exposure was associated with increased activation of extracellular signal-regulated protein kinase ERK 1/2. However, increased levels of phosphatase activity were observed following 8 h exposure. These findings suggest for the first time that organophosphorothionate pesticide-induced neurite retraction in N2a cells is associated with transient increases in NFH phosphorylation and ERK1/2 activation.

Keywords

Chlorpyrifos, Organophosphate toxicity, Neurite outgrowth, mouse N2a neuroblastoma cells, Neurofilaments, Microtubules, Neurotoxicity.

Introduction

Chlorpyrifos (CPF: chlorpyrifos, *O, O*-diethyl *O*-3,5,6-trichloropyridin-2-yl phosphorothionate, *O, O*-diethyl O-3,5,6-trichloro-2-pyridyl phosphorothionate, chlorpyrifos-ethyl) is one of the most extensively used organophosphate (OP) insecticides. It was introduced into the market in the 1960s, and is still used widely in agriculture and in the home. Following its entry into the body, CPF is metabolically converted into its oxygen or oxon analogue, in which the sulphur of its P=S group is replaced by oxygen. This biotransformation reaction is carried out mainly in the liver by the cytochrome P450 (CYP)-dependent monooxygenase system (Flaskos 2012). CPF activation to CPF-oxon (CPO) is the main cause of moderate acute toxicity in mammals (Richardson 1995).

Numerous *in vitro* studies using different cell culture models have reported the ability of CPF to induce neurodegenerative effects in animals and humans (Eaton et al. 2008; Flaskos et al. 2011). The principle mechanism of CPF toxicity involves the inhibition of acetylcholinesterase (AChE), which regulates neurotransmission at central and peripheral cholinergic synapses (Campbell et al. 1997; Steevens and Benson 1999). The persistent inhibition of AChE activity prevents acetylcholine (ACh) degradation, causing its accumulation, which can lead consequently to cholinergic overstimulation (Eaton et al. 2008; Flaskos 2012).

Severe cases of OP acute toxicity are defined by more than 70 % inhibition of AChE activity (Clegg and Gemert 1999a). Such cases develop a condition known as “cholinergic syndrome” which includes several CNS associated symptoms such as ataxia, coma, convulsion and blurred vision (Lotti 2005). However, in severe cases acute toxicity of OPs can cause respiratory failure, which is believed to be responsible for most fatalities in cases associated with CPF exposure (Larkin and Tjeedema 2000; Flaskos 2012). Furthermore, CPF poisoning can have a neurodegenerative effect on CNS neurons, especially in the spinal cord, resulting in a condition known as OP-induced

delayed neuropathy (OPIDN). In such cases, the primary target of this compound is the enzyme neuropathy target esterase (NTE), which has a crucial role in embryonic development and maintenance of peripheral axons (Lotti and Moretto 2005).

It has been shown that CPF and CPO can inhibit the outgrowth of neurites and disrupt the levels of cytoskeletal proteins in differentiating neuronal cell lines (Sachana et al. 2001, 2005; Flaskos et al. 2011). It is also known that the induction of developmental neurotoxicity may depend on the developmental stage at which exposure occurs. The majority of previous *in vitro* studies have involved the administration of OP at the point of induction of cell differentiation. However, little is known about the effects of OPs once cells have been committed to differentiation. The aim of the present study was to investigate the ability of non-cytotoxic concentrations of CPF and CPO to cause neurite retraction in pre-differentiated mouse N2a neuroblastoma cells and to relate these neurotoxic effects to the levels of expression and activities of cytoskeletal proteins and cell signaling pathways involved in neural cell differentiation and survival.

Materials and methods

Materials

The mouse N2a neuroblastoma cell line was purchased from ATCC-LGC Standards (Middlesex, UK). Cell culture plastic ware was supplied by SLS Laboratory Supplies (Nottingham, UK). Cell culture reagents were obtained from Lonza (Verviers, Belgium). Mouse monoclonal antibodies against total NFH (N52), phosphorylated NFH (SMI34), total α-tubulin (B512), GAP-43 (GAP-7B10) and β-III tubulin (2G10) were obtained from Sigma-Aldrich Co. Ltd. (Poole, UK). Rat anti-phosphorylated NFH (pNFH) monoclonal antibody (Ta51) was purchased from Chemicon Europe Ltd. (Chandlers Ford, UK). Mouse anti-phospho ERK 1/2 (E-4) and rabbit anti-total ERK 1/2 (K-23) were supplied by Santa Cruz Biotechnology (Santa Cruz, CA, USA). Horseradish peroxidase

(HRP) conjugated anti-rat and anti-mouse IgG secondary antibodies were purchased from DakoCytomation (Ely, UK). Chlorpyrifos and chlorpyrifos oxon (purity 97.6%) from Chem Service Inc. (West Chester, PA, USA), were supplied by Greyhound Chromatography (Birkenhead, UK). Unless otherwise stated, all other chemicals were obtained from Sigma-Aldrich Co. Ltd. (Poole, UK).

Cell Maintenance and the Induction of Cell Differentiation

Mouse neuroblastoma N2a cells were grown at 37°C in a humidified atmosphere of 5% CO_2/ 95% air and maintained as a monolayer in Dulbecco's modified Eagle's medium (DMEM) with 4.5 g/L glucose and 2 mM L-glutamine, supplemented with 10% (v/v) foetal bovine serum (FBS), penicillin (100 U/ml) and streptomycin (100 μg/ml). On reaching 60-80% confluence, cell cultures were either used to seed monolayers on 24 or 96 well plates for assays, T75 flasks for Western blot analysis or passaged to maintain the cell line. To passage the cell cultures, monolayers were mechanically removed from the flask surface by pipetting jets of growth medium and then harvested by centrifugation at 300 × g at room temperature for 5 min. The cells were then resuspended in DMEM by Pasteur pipette prior to sub-culture at the required cell density.

Only cells below passage number 20 were used in experiments. Cell differentiation was induced by serum withdrawal and the addition of 0.3 mM dibutyryl cyclic AMP (Flaskos et al. 2007). Prior to induction of differentiation, a viable cell count was determined using a haemocytometer chamber and Trypan blue exclusion assay (Bhuyan et al, 1976). Cells were then diluted to a density of 50,000 viable cells/ml, before 40 ml of cell suspension were seeded into each T75 culture flask.

After 24 h growth recovery, the growth medium was removed and replaced with serum free medium containing 0.3 mM dibutyryl cyclic AMP (differentiation medium). After 20 h of incubation, differentiation medium was replaced with the same volume of fresh differentiation

medium with or without CPF or CPO (at the final concentration indicated in Results). Cells were returned to the CO_2 incubator and incubated for a further 0.5 - 8 h, as appropriate. CPF and CPO were prepared as 200-fold concentrated stock solutions in dimethyl sulphoxide (DMSO) and added to the pre-warmed serum free medium immediately before use. Controls cells were treated with serum free medium containing the same concentration of DMSO (0.5% v/v).

Measurement of neurite outgrowth

Differentiated N2a cells were labeled using carboxyfluorescein succinimidyl ester (CFSE) fluorescent cell staining dye. Cells were seeded into 8-well cell chamber slides and induced to differentiate as indicated above. They were then incubated for 10 min with 10 μM CFSE dye in pre-warmed sterile phosphate buffered saline (PBS) before being treated with 3 μM CPF or CPO in differentiation medium at 37 °C. Cells were then fixed in pre-warmed 3.7% w/v formaldehyde in PBS, followed by three 10-min washes in PBS and mounted under glass cover slips using VectaShield® mounting medium for fluorescence (Vector Laboratories Ltd., Peterborough, UK) and viewed using an Olympus DP71 epifluorescence microscope. Eight culture wells were grown in four separate experiments. From each well, four random fields of view were selected giving a total cell count of 200-300 cells/well. In each field, the total number of cells and the total number of axon-like processes (long neurites; defined as extensions greater than two cell body diameters in length with an extension foot; Keilbaugh et al. 1991) were recorded and the mean number of long neurites per 100 cells was calculated (Flaskos et al. 1998).

High content analysis of neurite outgrowth

Alternatively, dose response experiments were performed using ibidi 8-well μ-slides seeded at 15,000 cells/well. Differentiated cell monolayers were exposed for 8 h in the presence and absence of 1, 3 and 10 μM CPF or CPO, after which they were fixed and stained with monoclonal antibodies to total α-tubulin (B512) or to pNFH (Ta51), as described below for indirect

immunofluorescence. The effects of OP exposure on neurite outgrowth were detected using an ImageXpress® Micro Widefield High Content Screening (HCS) System (Molecular Devices, Wokingham, UK).

Fluorescence images were acquired using a 10× objective lens and then analysed by MetaXpress software, using Neurite Outgrowth analysis settings. Objects were identified as cells if valid nuclei had been detected and cell body width ranged from 10 to 25 μm. Outgrowths longer than 10 μm were recorded as neurites. Analysis was performed on a total of 4 fields and at least 200 cells per well from four independent experiments. The maximum neurite length per cell (i.e. the average of the maximum neurite length recorded for each cell in a field) or the average neurite length per cell (i.e. the average of all recorded neurite lengths for each cell in a field) were recorded.

Cell Viability Assessment

The effects of CPF and CPO (1, 3 and 10 μM) on the viability of N2a cells were determined by the 3-(4,5-dimethylthiazol-2-yl)-2,5 diphenyltetrazolium bromide (MTT) reduction assay (Mosmann 1983). For this, cells were plated out in Corning 24 well plates. At 30 min prior to the end of the required incubation period, a volume of 50 μl MTT (5 mg/ml solution in DMEM) was added to each culture well and re-incubated for 30 min at 37°C. Differentiation medium was then aspirated and DMSO was added to solubilise the reduced formazan crystals, the absorbance of which was read at 570 nm. There was no significant effect on MTT reduction compared to untreated controls at any of the OP concentrations tested (not shown).

Acetylcholinesterase Activity Assay

For this, 2 million cells were plated into T75 culture flasks and induced to differentiate as above. Cells were harvested by centrifugation, resuspended in ice-cold PBS and transferred into an Eppendorf micro-centrifuge tube. Cells were micro-centrifuged at 10,000 × g for 3 min to remove traces of DMEM. Cell pellets were then resuspended in ice cold 200 mM sodium phosphate buffer (pH 7.4) containing Triton X100 (0.1% v/v) at 4°C. AChE was then determined according to the assay of Ellman et al. (1961) modified for a microtitre plate format, as described by Flaskos et al. (2007).

Indirect Immunofluorescence

The intracellular distribution of neurofilaments and microtubules was further studied by indirect immunofluorescence staining. Initially, N2a cells were seeded into an 8-well cell culture chamber slide for 24 h, after which they were induced to differentiate with or without OPs as described earlier. N2a cells were fixed for 10 min with 3.7% w/v formaldehyde in PBS, extracted in 0.5% w/v Tween-20 in Tris buffered saline (TBS: 10 mM Tris, 140 mM NaCl; pH 7.4) for 15 min and blocked with 3 % w/v bovine serum albumin (BSA) in TBS (BSA/TBS) for 45 min at room temperature. They were then incubated with primary antibodies against NFH, p-NFH and β-tubulin followed by Alexa Fluor 488 rabbit anti-mouse IgG labeled secondary antibody, as described previously (Hargreaves et al. 2006; Harris et al. 2009b; Flaskos et al. 2007, 2011). After washing, to remove unbound secondary antibodies, the chamber slide was carefully dismantled and the cell monolayer mounted under a glass coverslip using VectaShield® mounting medium for fluorescence (Vector Laboratories Ltd., Peterborough, UK) containing DAPI counterstain for nuclei visualization. Finally, the slide was viewed using an Olympus DP71 epifluorescence microscope system.

Live Cell Imaging

The real time changes in cell morphology following toxin exposure were determined using CFSE and monitored using a Leica TCS SP5 confocal laser scanning microscope with epifluorescence optics. The N2a cells were incubated in an environmental chamber which controlled the temperature and CO_2. They were seeded into 96-well black-sided cell culture treated plates (BD Falcon™), induced to differentiate and labeled with CFSE prior to OP exposure, as described earlier. For each well, the focal point of the microscope lens was set to the position where cells with clear axons were detected. Non-treated live cells were first imaged to create a time zero measurement before adding the toxins. After that, a 3 μM concentration of CPF or CPO was added to each treatment well and the same positions were viewed every 30 min for an interval of 8 h exposure time. Live image snapshots were then obtained using Leica application suite advanced fluorescence lite (LAS AF) and selected axons were detected and measured.

Gel Electrophoresis and Western Blot Analysis

For Western blotting analysis, N2a cells were seeded and induced to differentiate, then treated in the presence and absence of CPF or CPO compounds for up to 8 h in T75 culture flasks, as described above. Intact cell monolayers were then solubilised by boiling in 2 ml of 0.5% w/v sodium dodecyl sulphate (SDS) in TBS prior to protein estimation. Protein was estimated by the bicinchoninic acid (BCA) assay, using BSA as the standard (Brown et al. 1989). The resultant cell lysates were subsequently subjected to gel electrophoresis in the presence of SDS (SDS-PAGE) employing a 10% w/v polyacrylamide resolving gel overlaid with a 4% w/v polyacrylamide stacking gel (Laemmli 1970). Separated proteins were then electrophoretically transferred onto nitrocellulose membrane filters (Towbin et al. 1979). The resultant Western blots were blocked with BSA/TBS for at least 1 h at room temperature. Blots were then probed overnight at 4°C with appropriate dilutions of primary antibodies in BSA/TBS, including mouse anti-total NFH (N52, dilution 1:250), rat anti-pNFH (Ta51, dilution 1:250), anti-GAP-43 (GAP7B10, dilution 1:1000),

mouse anti-α-tubulin (B512, dilution 1:2000), mouse anti-β-III tubulin (2G10, dilution 1:1000), mouse anti-phosphorylated ERK 1/2 MAP kinase (E-4, dilution 1:500), monoclonal antibodies and the rabbit-total ERK 1/2 (K-23, dilution 1:1000). After six 10-min washes in TBS containing 0.05% v/v Tween-20 (TBS/Tween), blots were probed with horseradish peroxidase (HRP)-conjugated secondary antibodies for 2 h at room temperature. Following 6 further washes with TBS/Tween, antibody reactivity was visualized using enhanced chemiluminescence (ECL) reagent (Thermo Scientific, Rockford, IL, USA). For quantification of antibody reactivity, band intensities on images of developed Western blots were determined using Advanced Image Data Analysis software (AIDA; Fuji). All band densities were normalized to that of anti-α-tubulin, which was used as internal control.

Enzyme-linked immunosorbent assay (ELISA) of fixed cell monolayers

For concentration-response experiments, cells were seeded in sterile flat-bottomed 96-well culture dishes at a density of 50,000 cells/ml in a total volume of 200 µl growth medium per well (four replicates) and incubated overnight in a CO_2 incubator. After 24 h recovery, cells were induced to differentiate for 20 h, as described earlier, after which they were treated in the absence or presence of OP at final concentrations of 1, 3, and 10 µM in fresh differentiation medium for 2 or 8 h. Serum-free medium was then removed by aspiration and cell monolayers were fixed by pre-warmed 4% (w/v) paraformaldehyde (Sigma-Aldrich, UK) (200 µl/well) for 10 min at room temperature. Fixative was then removed and the plate was washed twice with 200 µl/well of ice-cold TBS (2 min/wash). Next, cells were incubated in permeabilisation buffer (0.5% (v/v) Tween-20 in TBS) for 15 min at room temperature, after which they were rinsed twice with TBS. A volume of 300 µl/well of BSA/TBS was then applied and the plate was incubated overnight at 4°C. The blocking buffer was then removed and 100 µl/well of primary antibodies diluted 1:1000 in BSA/TBS were added and incubated overnight at 4°C.

After removing the primary antibodies, wells were washed again twice with TBS/Tween, followed by 2 h incubation in 200 µl/well of diluted HRP-conjugated secondary antibodies at room temperature. After removal of secondary antibodies, two final washes were applied with TBS/Tween 20. The reaction was started by the addition into each well of 100 µl developing buffer (100 mM sodium acetate buffer pH 6, containing 0.075 mg/ml tetra methyl benzidine and 0.005 % v/v H_2O_2). After 5 min incubation at room temperature, colour development was stopped by the addition of 100 µl of 5 M sulphuric acid. Absorbance was measured at a wavelength of 450 nm using an ASYS Expert 96 microtitre plate reader (Biochrom, UK).

Phosphatase Assay

The activity of alkaline phosphatase was monitored using the p-Nitrophenyl Phosphate (pNPP) liquid substrate system. Cells were seeded and induced to differentiate in the presence and absence of OPs in T75 culture flasks, as described above, after which they were harvested by centrifugation, resuspended in 1 ml ice-cold PBS (pH7.4) and transferred into Eppendorf tubes. All tubes were then micro-centrifuged at 10,000 × g for 3 min. Cell pellets were resuspended in ice cold TBS containing 0.5% v/v Triton X100. Cell pellets were broken down by gentle pipetting and transferred into a 96-well microtitre plate (50 µl/well). The reaction was started when 100 µl of pNPP liquid substrate system were added into each well. The absorbance was then recorded at regular intervals for 30 min at 405 nm in a microtitre plate reader. Protein was estimated in the retained 100 µl of cell lysate by the BCA assay (Brown et al. 1989), and specific activity was expressed as absorbance change /mg protein/h.

Statistical Analysis

All sets of quantitative data were based on a minimum of 4 separate experiments and expressed as mean ± SEM. Average values for each treatment were compared to the corresponding control by one-way or two-way ANOVA, as appropriate, using 95% confidence limits. Differences were

considered to be statistically significant when $p < 0.05$. GraphPad Prism 6 software was used for the production of graphs and statistical analysis.

Results

In a preliminary study we found that CPF at a non-cytotoxic concentration of 3μM had the ability to induce retraction of approximately 50 % of axon-like processes formed by differentiating N2a cells, as determined by Coomassie Brilliant Blue staining (Sachana et al. 2001). However, the effects of CPO on pre-formed neurites had not been previously tested. In order to achieve comparable results to the previous work with CPF, live N2a cells were stained directly with CFSE dye and the growth of long neurites was recorded for each exposure time point under similar conditions. In the current study, it was clearly shown that exposure of pre-differentiated N2a cells to 3 μM CPF and CPO significantly reduced the numbers of axon-like processes compared to non OP-treated controls in a time dependent manner (Fig. 1 and 2a), CPO being slightly more toxic than CPF. However, MTT reduction assays showed no significant effect of these OPs on the viability of N2a cells under the same experimental conditions (not shown). The concentration-response relationship of this effect was then further studied for each compound using high content analysis (HCA) of immunofluorescently-stained cell monolayers after 8 h exposure to each OP at a concentration of 1, 3 or 10 μM. As can be seen in Fig. 2b, there was a dose-dependent decrease in both the maximum and average neurite length per cell, in fixed cell monolayers stained with monoclonal antibodies B512 and Ta51 to detect total α-tubulin and phosphorylated NFH, which are indicative of total and axon-like neurites, respectively. The reductions in average neurite length were similar for both compounds. However, the reduction in maximum neurite length in Ta51- but not B512-stained cell monolayers was greater in CPO-treated cells.

The impact of 3 μM CPF and CPO on the activity of AChE enzyme in differentiating N2a cells was further assessed to determine whether the morphological changes in the outgrowth of neurites could

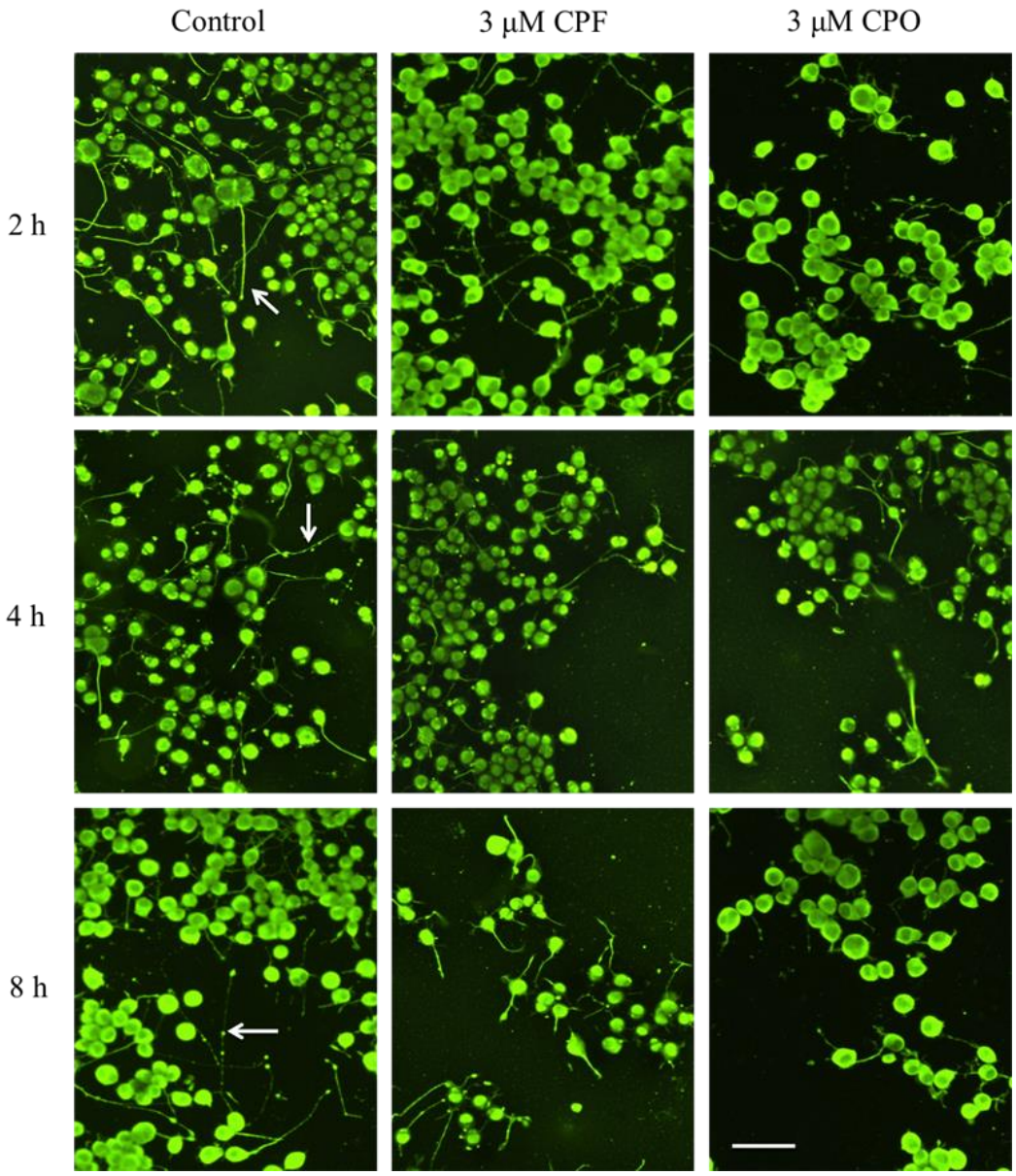

Figure 1: Effects of 3 µM CPF and CPO on the morphology of pre-differentiated N2a cells. Displayed are representative fluorescence images of N2a cells induced to differentiate for 20 h prior being incubated in the absence (Control) or presence of 3 µM CPF or 3 µM CPO for 2, 4 and 8 h. Cells were stained with CFSE and fixed. Arrows show typical axon-like processes detected in non-OP treated controls. Scale bar represents 50 µm.

be related to AChE inhibition. As illustrated in Fig. 3, after 0.5, 2, 4 or 8 h exposure, 3 µM CPO - treated cells showed a sustained significant reduction (>70 %) in the specific activity of AChE compared to non OP-treated controls ($p<0.05$), whereas the same concentration of CPF showed little or no effect.

The neurotoxic effects of both CPF and CPO on the intracellular distribution of microtubules and neurofilaments were then monitored using immunofluorescence staining of N2a cells after 4 and 8 h

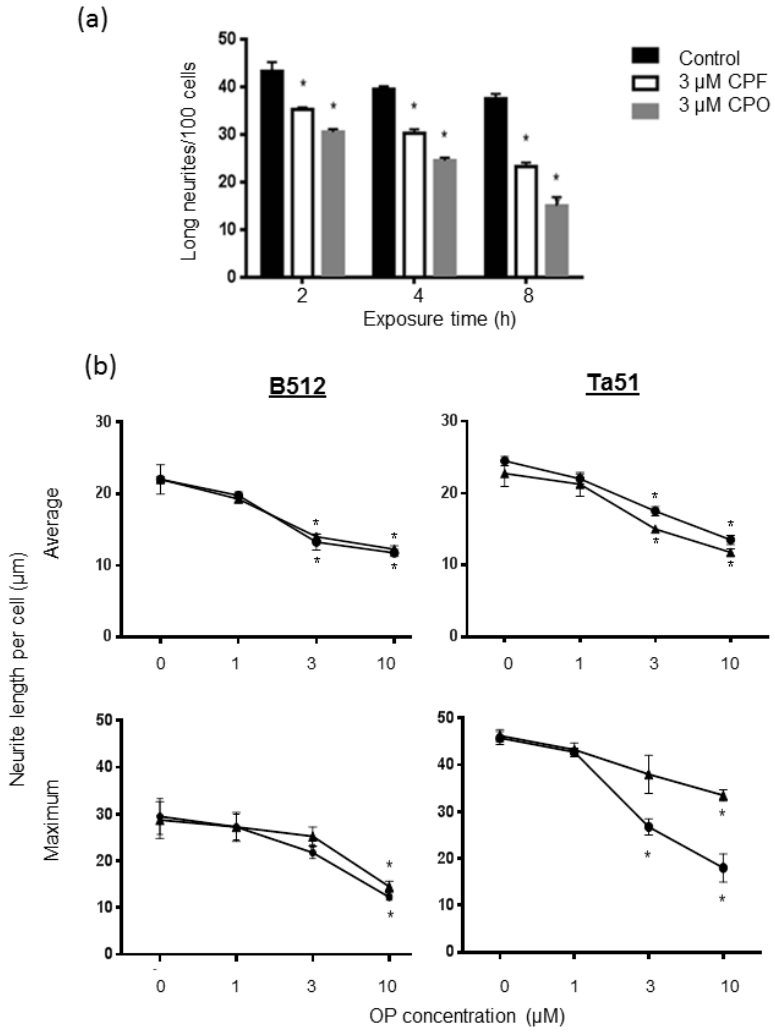

Figure 2: Quantitative analysis of the effects of CPF and CPO on neurite outgrowth. Mouse N2a neuroblastoma cells were induced to differentiate for 20 h, as described in Materials and methods. They were then either (a) labeled with CFSE then incubated in the absence or presence of 3 µM CPF and CPO for 2, 4, and 8 h or (b) treated for 8 h with 0-10 µM CPF (triangles) or CPO (circles) prior to fixation and indirect immunofluorescence staining with antibodies to total α-tubulin (B512) or pNFH (Ta51). Data from 4 independent experiments are expressed as (a) mean number of long neurites per 100 cells ± SEM or (b) average/maximum neurite length per cell ± SEM. Asterisks indicate where OP-treated cell values were significantly different from the corresponding control ($p<0.05$).

exposure. In the case of neurofilaments, it can be seen that there was relatively strong staining of axons in control cells; much less neurite staining was observed in CPF and CPO treated N2a cells, where more aggregates were observed in cell bodies. In the case of anti-β-III tubulin, intense staining was detected both in cell bodies and in remaining neurites of both OP-treated and non OP-treated cells (Fig. 4).

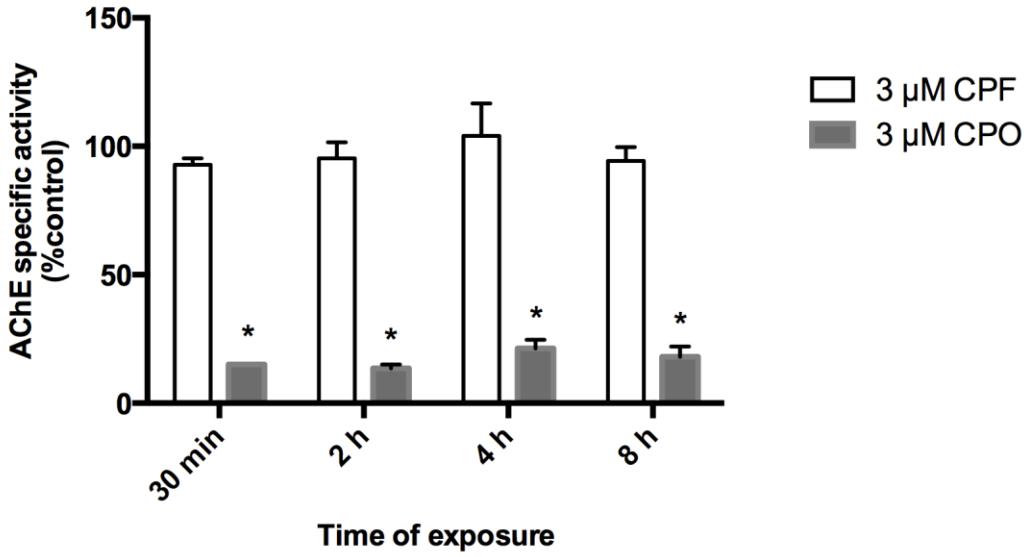

Figure 3: Effects of non-cytotoxic concentrations of CPF and CPO on acetylcholinesterase activity in differentiating N2a cells. N2a cells were induced to differentiate for 20 h before being incubated with or without 3 µM of CPF and CPO for 0.5, 2, 4 and 8 h, after which the activity of AChE was measured as described in Materials and methods. Control specific activities were within the range 0.70 ± 0.06 absorbance units/mg protein/min. Results are expressed as mean specific activity (% control) ± SEM from 4 separate experiments. Asterisks show statistically significant changes compared to the control values (p<0.05).

In order to determine the real time effects of toxins on N2a cell morphology, a live cell imaging approach was developed. Images were recorded at 30 min intervals for a period of 8 h from the addition of toxin. Neurite length was shown to be highly affected over time. Approximately 25 % of neurites retracted within the first 2 to 4 h, suggesting that some of these changes were occurring at a very early stage. However, no other variations in cell morphology were detected, such as changes in cell body shape or size (Fig. 5). Time lapse videos of control and CPO-treated cells are shown in Supplementary Data, figures 1 and 2 (available via online access at journal website).

The molecular changes underlying the neurotoxic effects of these compounds on the maintenance of neurites in pre-differentiated N2a cells were further studied by quantitative Western blotting using antibodies against a range of cytoskeletal and axon growth associated proteins. As indicated in Fig. 6a and Table 1, there were no significant changes in the cross reactivity of N2a cell lysates with antibodies against α-tubulin (B512) following exposure to 3 µM CPF and CPO at all of the time points. A transient reduction was observed in the levels of GAP-43 (GAP7B10) after 4 h of exposure in cell lysates treated with both compounds. However, GAP-43 reactivity was unaffected

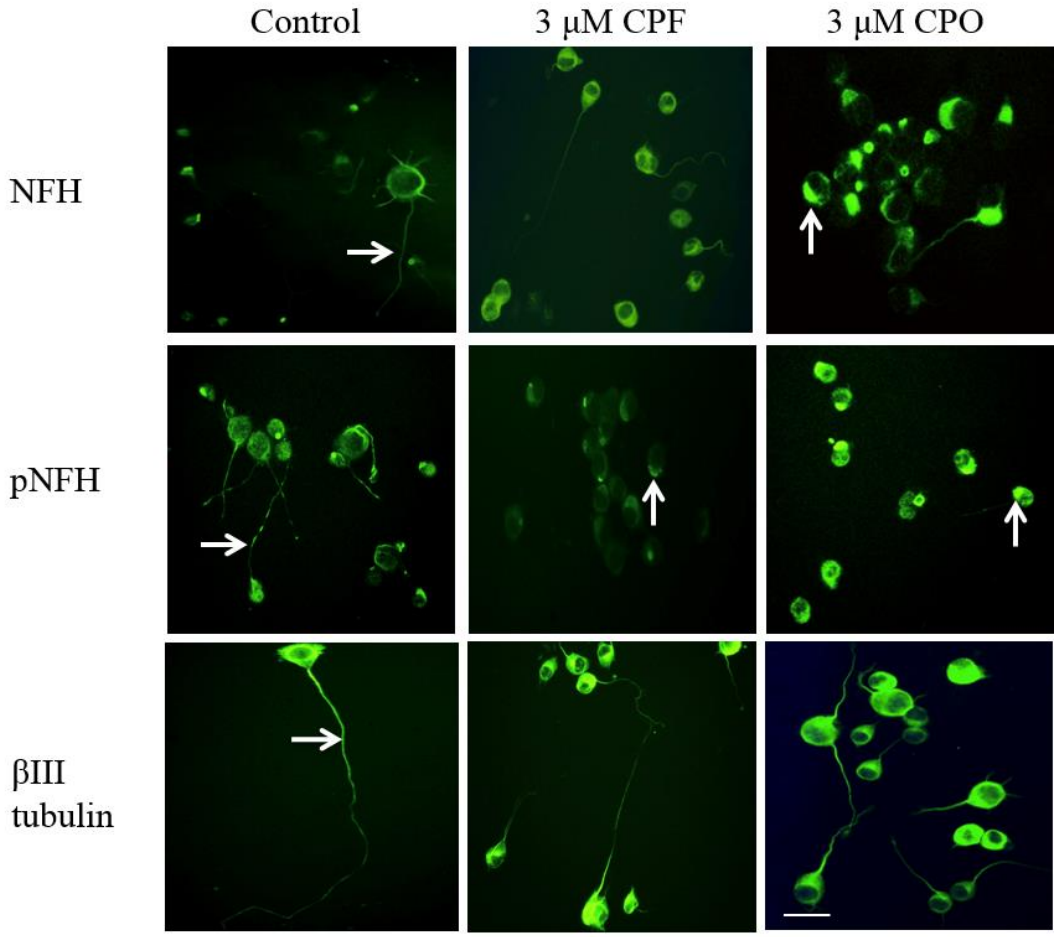

Figure 4: Immunofluorescence staining of differentiating N2a cells. Cells were induced to differentiate for 20 h prior to being treated with or without 3 μM of CPF or CPO for 8 h. Cells were then fixed and stained by indirect immunofluorescence as described in Materials and methods. Shown are digital images of non OP-treated control and cells exposed to 3 μM CPF or 3 μM CPO stained with anti-NFH (N52), anti-phosphorylated NFH (SMI34) and anti-βIII tubulin (2G10). Horizontal arrows display typical axon-like neurites and vertical arrows show aggregates in cell bodies. Bar represents 30 μm.

following exposure to both agents for 2 h and seemed to recover following 8 h of exposure. Reactivity of cell extracts with anti-total NFH (N52) antibody was similar to the corresponding control at all of the time points. In contrast, reactivity with anti-pNFH (Ta51) was considerably higher than the reactivity level of non-OP treated control at 2 h, which was then followed by a significant decline in comparison to control values at 8 h exposure to both compounds. Similar responses were also found for B512 and Ta51 reactivity using a cell ELISA approach, the effects being dose-dependent over the 1-10 μM concentration range (Fig. 6b).

Further analyses were performed to determine whether the altered levels of reactivity of lysates with antibodies to pNFH could be attributed to changes in the activation status of extracellular

Antigens	Incubation time (h)	Densitometric peak area (%control ± S.E.M.)	
		3µM CPF	3µM CPO
NFH	2	107±9	101±8
	4	102±18	81±22
	8	120±12	105±16
pNFH (Ta51)	2	214±16*	444±90*
	4	84±7	93±12
	8	36±4*	30±1*
Total α-tubulin	2	107±8	96±7
	4	102±5	102±8
	8	103±6	106±7
GAP-43	2	107±12	96±5
	4	75±6*	60±10*
	8	106±11	117±17

Table 1: Densitometric analysis of Western blots probed with antibodies to cytoskeletal and growth associated proteins. N2a cell lysates were induced to differentiate for 20 h prior to being treated with or without 3 µM of CPF or CPO for 2, 4 and 8 h. They were then subjected to SDS-PAGE and Western blotting analysis using antibodies that recognise NFH, pNFH (Ta51), total α-tubulin and GAP-43. Shown are data from 6 separate experiments. Band densities were normalized to anti-α-tubulin. Data are expressed as a percentage of their corresponding control ± SEM. Asterisks indicate values that were statistically significant from their corresponding control (p<0.05).

signal-regulated protein kinase ERK 1/2, which is known to be important in neurite outgrowth and phosphorylation of NFH (Perron and Bixby 1999). Data from Western blotting analyses using anti-total ERK showed no significant changes in reactivity levels with lysates from N2a cells treated with either CPF or CPO compared to non OP-treated controls. In contrast, anti-pERK antibodies showed increased reactivity compared to the corresponding control at all of the time points but the changes were only statistically significant at 2 h exposure (Fig. 7a and Table. 2). Measurements by cell ELISA showed a similar pattern of ERK activation, which was concentration dependent and stronger for CPO than for CPF (Fig. 7b).

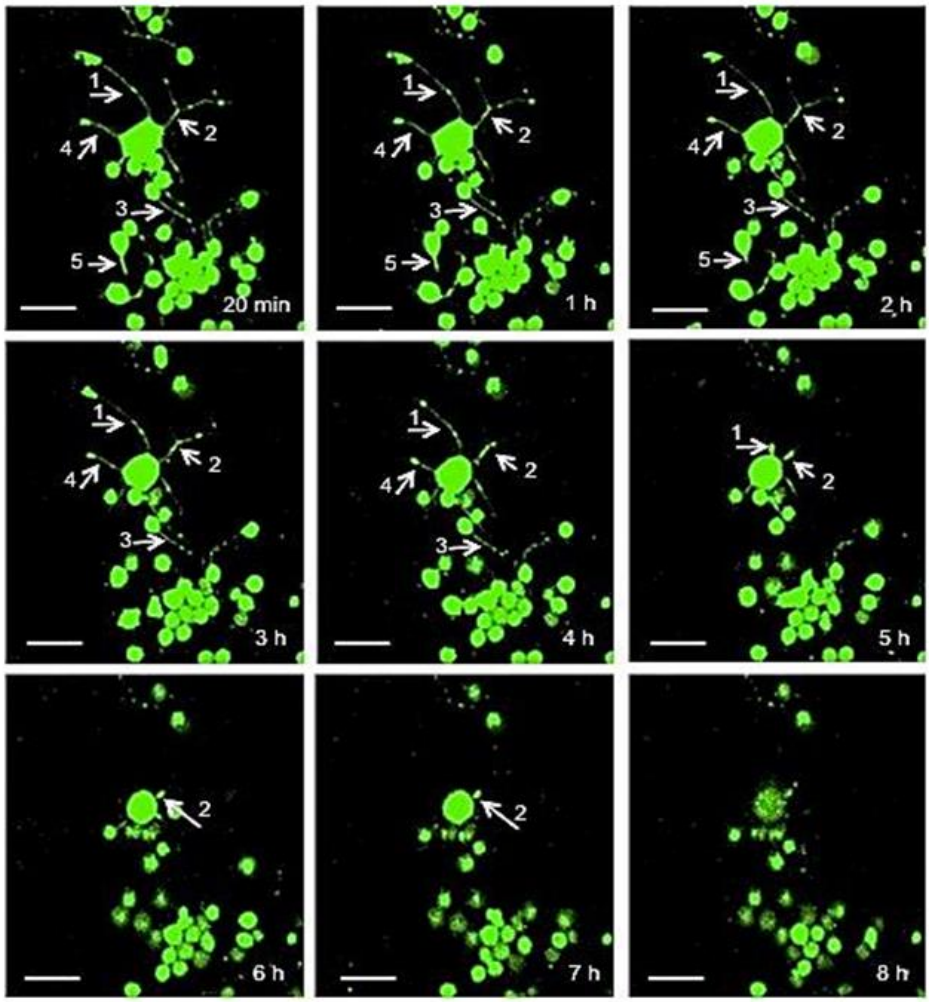

Figure 5: Live cell imaging of differentiating N2a cells. Cells were induced to differentiate for 20 h, stained with CFSE then treated with 3 μM of CPO prior to analysis as described in Materials and methods. Shown are digital images of snapshots taken of treated cells at the same location. The real time changes in cell morphology following toxin exposure were recorded for a period of 8 h, the first image being taken at minute 20. Subsequent images were taken 1 h intervals, using a Leica TCS SP5 confocal laser scanning microscope with epifluorescence optics. Arrows labeled 1-5 show retracting neurites detected in differentiating N2a cells and scale bar represents 30 μm.

Since there was a clear relationship between the early changes in reactivity of antibodies against pNFH and pERK activity in OP-treated cell lysates, further experiments were carried out to detect the possible cause for the subsequently observed reductions pNFH phosphorylation following 4 and 8 h exposure. For this, phosphatase activity was detected using pNPP liquid substrate under the same experimental conditions. As demonstrated in Fig. 8, phosphatase activity in control cells increased from 2 to 4 h then stabilized. This effect may be the consequence of the addition of fresh medium. There was a significant increase relative to the controls in the level of phosphatase activity in extracts from cells treated with either CPF or CPO for 8 h. However, at 2 and 4 h treatment no

statistically significant changes were detected in lysates from OP-treated cells (Fig. 8

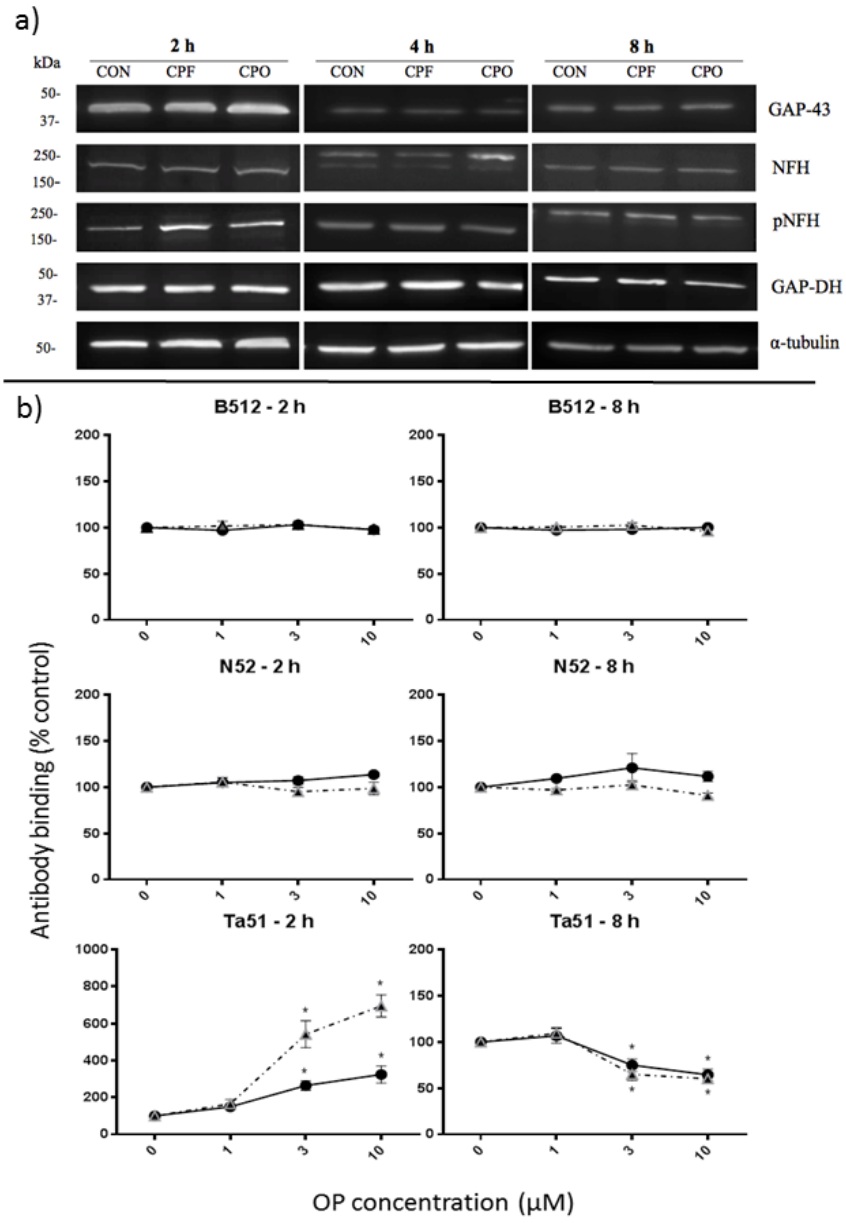

).

Figure 6: Detection of cytoskeletal proteins by Western blot analysis and cell-ELISA. For the data shown in panel A) cells were induced to differentiate for 20 h prior to treatment without (CON) or with 3 μM CPF (CPF) or 3 μM CPO (CPO) for 2, 4 and 8 h, after which cell lysates were subjected to SDS-PAGE and Western blotting as described in Materials and methods. Shown are typical blots probed with antibodies to NFH (N52), pNFH (Ta51), α-tubulin (B512) and GAP-43 (GAP7B10) followed by HRP-conjugated secondary antibodies and developed by ECL reagents. Alternatively, as shown in panel B), cells were differentiated as described above then exposed to CPF (circles) or CPO (triangles) at the concentrations indicated, before being fixed and stained with monoclonal antibodies B512, N52 and Ta51 and their reactivity with monolayers quantified by ELISA as described in Materials and methods. Data are presented a percentage of the non OP-treated control ± SEM from four independent experiments. Data were analysed using two way ANOVA. CPF effects are shown by blue solid lines with circles; CPO effects are shown as red dashed lines with triangles. Asterisks indicate changes that are statistically different from the non OP-treated controls ($p < 0.05$). When SEM bars are not visible, the error is smaller than the symbol size.

Discussion

The data presented on neurite outgrowth in CFSE-labeled cells and HCA of cells stained with monoclonal antibodies B512 and Ta51 demonstrated that both CPF and CPO caused neurite

retraction in a dose and time dependent manner when administered to pre-differentiated N2a cells. As indicated earlier, B512 stains all neurites (i.e. both axon- and dendrite-like processes) whereas

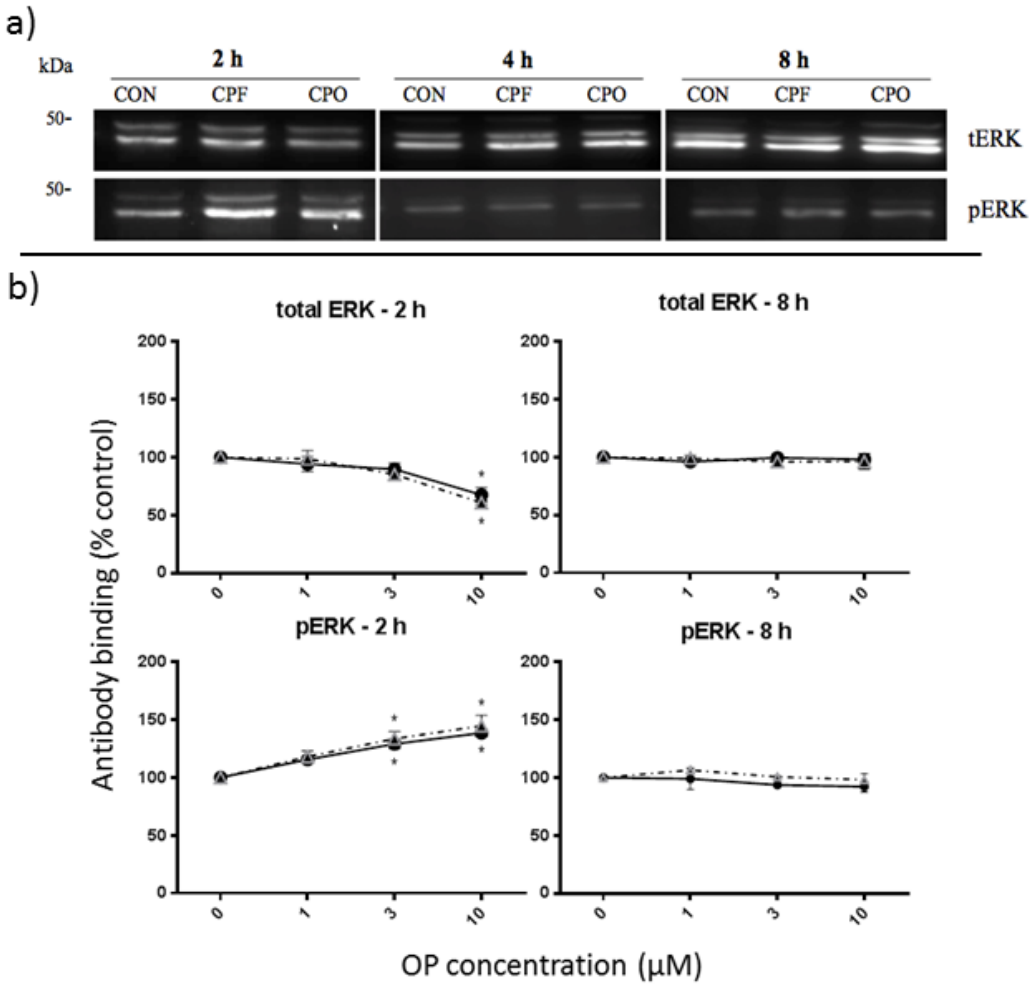

Figure 7: Detection of cell signaling proteins by Western blot analysis and cell-ELISA. For the data shown in panel A), cells were induced to differentiate for 20 h prior to treatment without (CON) or with 3 µM CPF (CPF) or 3 µM CPO (CPO) for 2, 4 and 8 h then cell lysates were subjected to SDS-PAGE and Western blotting as described in Materials and methods. Shown are typical blots probed with antibodies to total ERK 1/2 (K-23) and phosphorylated ERK 1/2 MAP kinase (E-4), followed by HRP-conjugated secondary antibodies and developed by ECL reagents. Alternatively, as shown in panel B), cells were differentiated as described above then exposed to CPF (triangles) or CPO (circles) at the concentrations indicated, before being fixed and stained with monoclonal antibodies to total and pERK, after which their reactivity with monolayers quantified by ELISA as described in Materials and methods. Data are presented a percentage of the non OP-treated control ± SEM from four independent experiments. Data were analysed using two way ANOVA. CPF effects are shown by blue solid lines with circles; CPO effects are shown as red dashed lines with triangles. Asterisks indicate changes that are statistically different from the non OP-treated controls ($p < 0.05$). When SEM bars are not visible, the error is smaller than the symbol size.

Ta51 stains pNFH, which is enriched in axons. Therefore, the observation that the average and maximum lengths of neurites in cells stained with Ta51 were greater than the same values for B512 stained cells is consistent with the view that a significant proportion of longer neurites in differentiating N2a cells are axon-like (Keilbaugh et al., 1991; Sachana et al. 2003; Hargreaves et

Antigens	Incubation time (h)	Densitometric peak area (%control ± S.E.M.)	
		3μM CPF	3μM CPO
Total ERK	2	106 ± 7	95 ± 11
	4	111 ± 14	115 ± 20
	8	107 ± 7	107 ± 8
pERK	2	147 ± 21*	128 ± 6*
	4	149 ± 33	142 ± 34
	8	113 ± 15	91 ± 2
Total α-tubulin	2	106 ± 9	98 ± 5
	4	104 ± 2	107 ± 9
	8	102 ± 7	104 ± 9

Table 2: Densitometric analyses of Western blots probed with antibodies to cell signaling proteins. N2a cell lysates were induced to differentiate for 20 h prior to being treated with or without 3 μM of CPF or CPO for 2, 4 and 8 h. They were then subjected to SDS-PAGE and Western blotting analysis using antibodies that recognise total ERK 1/2 (K-23) and phosphorylated ERK 1/2 MAP kinase (E-4). Shown are data from 6 separate experiments. Band densities were normalized to anti-α-tubulin (B512 reactivity). Data are expressed as a percentage of their corresponding control ± SEM. Asterisks indicate values that were statistically significant from their corresponding control (p<0.05).

al. 2006; Harris et al. 2009b; Flaskos et al. 2007; 2011). The trend of greater reduction in the number of long neurites and the maximum neurite length observed in Ta51-stained CPO-treated cells is consistent with the possibility that the oxon metabolite may have a greater impact or a more

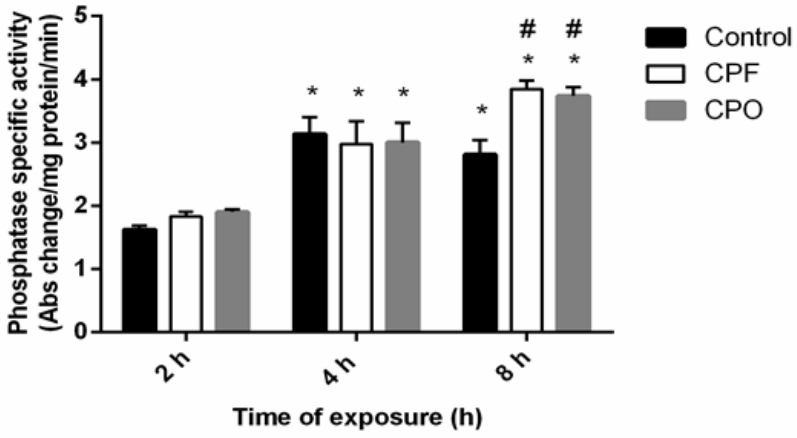

Figure 8: Effects of CPF and CPO on phosphatase activity in differentiating N2a cells. Cells were induced to differentiate for 20 h prior to being treated with or without 3 μM CPF or CPO for 2, 4 or 8 h. Data are expressed as mean specific activity (absorbance change/mg protein/h) ± SEM for 4 separate experiments. Asterisks in the 8 h treatment demonstrate changes that are significantly different to the non OP treated control (p<0.05). # indicates significant increases relative to the 2 h non OP treated control

rapid effect on the retraction of axon-like processes than the parent compound under the exposure conditions tested.

Although inhibition of neurite outgrowth from N2a cells has been previously investigated after CPF exposure (Sachana et al. 2001), and other OPs such as leptophos, phenyl saligenin phosphate (PSP), diazinon and CPO using Coomassie blue staining (Sachana et al. 2003; Hargreaves et al. 2006; Harris et al. 2009b; Flaskos et al. 2007; 2011), this is the first time that CFSE has been used to measure the growth or retraction of neurites in cultured N2a cells. Since it provides similar results to our previous work with CPF, morphometric analysis of CFSE-labeled N2a cells can be considered as a novel and reliable approach to assess cell differentiation and neurite outgrowth. Furthermore, the data from HCA not only confirm the validity of our previously used manual approach to morphological assessments, they additionally illustrate the concentration dependence of the effects of these OPs on neurite retraction.

The observed retraction of neurites induced by CPF on pre-differentiated N2a cells (i.e. under post-differentiation exposure conditions) is in good agreement with that noted in the same culture system using a similar concentration of CPF under both post- and co-differentiation conditions (Sachana et al. 2001). In addition, the current study has revealed for the first time the potential neurotoxic ability of CPO to induce the retraction of axon-like processes from pre-differentiated N2a cells, and that this effect appears to be stronger than that of CPF with respect to longer (axon-like) neurites. The rapid collapse of neurites observed in experiments using live cell imaging further confirms the neurite destabilising effect of CPF and CPO towards pre-differentiated N2a cells (Fig 5), since all neurites, irrespective of initial size, exhibited reduced lengths from within 2h of exposure to both compounds..

The inability of either compound to affect MTT reduction suggested that the concentrations used in this study were non-cytotoxic towards pre-differentiated N2a cells. This finding is in agreement

with previous studies which employed similar concentrations (1-10 μM) of CPF and other OPs such as diazinon and diazinon oxon that were also found to be non-cytotoxic towards differentiating N2a cells for exposure periods of up to 24 h (Flaskos et al. 2007; Sachana et al. 2001, 2003, 2005; Sidiropoulou et al. 2009). However, in those studies exposure was initiated at the point of induction of cell differentiation (i.e. under co-differentiation conditions).

The significant reduction in the specific activity of AChE observed at all time-points of CPO exposure is in line with a previous study by Flaskos et al. (2011), which demonstrated sustained inhibition of AChE in differentiating N2a cells that were exposed for 4 or 24 h to CPO from the point of induction of cell differentiation. A reduced activity of AChE was also noted in N2a cells exposed for 4 h from the point of induction of differentiation to the OP diazoxon, although in that case no significant effect was observed after 24 h (Sidiropoulou et al. 2009). However, it is unlikely that inhibition of AChE alone could account for the morphological changes in the outgrowth of neurites in N2a cells, as CPF (as would be expected) had little effect on AChE in the current work, and a number of *in vivo* (Slotkin et al. 2006) and *in vitro* (Das and Barone 1999; Fowler et al. 2001; Howard et al. 2005) studies suggest that OPs capable of only weak inhibition of AChE can also induce marked impairment in the development of neurites. In this respect, the OP trio-ortho-cresyl phosphate significantly inhibited the development of axon-like processes in N2a cells. However, it is only a weak inhibitor of AChE (Lock and Johnson 1990). Therefore, inhibition of AChE activity by CPF or CPO is unlikely to be the main cause of retraction of axon-like neurites in N2a cells, although our data suggest that high levels of cholinesterase inhibition may increase the severity of certain OP effects on neurite outgrowth.

Indirect immunofluorescence findings further confirmed the idea that both compounds could impair neurite development and interfere with the expression levels and/or intracellular distribution of cytoskeletal proteins. The changes in the staining intensity from clear axonal staining in the control

cells to aggregates in the cell bodies of treated cells, suggested that the neurofilament network was heavily disrupted by CPF and CPO treatments. This disruption in the intracellular distribution of neurofilaments is consistent with that observed in previous studies, in which cells were induced to differentiate for 24 h in the presence and absence of non-cytotoxic neurite inhibitory concentrations of phenyl saligenin phosphate (Hargreaves et al. 2006), diazinon (Flaskos et al. 2007) and CPO (Flaskos et al. 2011). On the other hand, the similar distribution of anti-tubulin staining in cell bodies and neurites of OP-treated and control cells indicated no major disruption of the microtubule network, suggesting that microtubules are not the main target for OP pesticides in differentiating N2a cells.

Neurofilaments play a key role in regulating axon girth and stability (Williamson et al. 1996) and are increasingly expressed and phosphorylated as axons develop (Lee et al. 1988; Veerana et al. 1998). Thus, it was of interest to determine whether inhibition of neurite outgrowth could be reflected at the molecular level by altered levels of phosphorylation of NFH. The observed increase in the reactivity of antibodies against pNFH in OP-treated cell lysates at 2 h and the following decline at 8 h exposure, together with the lack of statistically significant effects of OPs on the reactivity of antibodies that recognise total NFH at all time-points are consistent with an early transient hyperphosphorylation of NFH followed by a reduced phosphorylation state of NFH, with no overall effect on the total levels of NFH protein. The data for CPF are in agreement with an earlier study, which revealed little or no effect on the levels of NFH from N2a cells following exposure to CPF under similar post differentiation conditions (Sachana et al. 2001). However, in our previous work, when CPF and CPO were added to N2a cells at the same time as induction of differentiation, immunoblot analysis indicated significant reduction in NFH protein but the level of NFH phosphorylation remained close to the control values (Flaskos et al. 2011), suggesting that the effect observed in the current work was specific for pre-differentiated cells. Thus, the toxicity

response may be related to the developmental stage of cell differentiation at which the exposure to OPs occurs.

The observation that densitometric analysis revealed no change in the reactivity of N2a cell lysates with antibodies against α-tubulin following treatment with either compound is consistent with the strong staining patterns of remaining neurites with anti-βIII tubulin antibody obtained by indirect immunofluorescence, suggesting that the microtubule network was not a primary target of OPs. This view is also supported by previous studies, which found no detectable changes in the level of total α-tubulin after co-differentiation exposure of N2a cells to other OP compounds (Hargreaves et al. 2006; Flaskos et al. 2007, 2011; Sidiropoulou et al. 2008, Harris et al. 2009a). These data, together with the findings presented in the current study, suggest that altered tubulin levels are not associated with neurite inhibitory effects of CPF and CPO towards differentiating N2a cells.

Results obtained from immunoblot analysis using monoclonal antibody GAP7B10 suggested that CPF and CPO induced a transient reduction in GAP-43 levels after 4 h exposure. This protein is highly expressed in axons during elongation and has been shown to play a vital role in axon outgrowth and maintenance (Skene 1989); since reduced levels of GAP-43 occurred in parallel with the observed collapse in axon outgrowth obtained by live cell imaging, it could also have contributed to the detachment of the growth cones. Previously, reduced levels of GAP-43 were also reported in N2a cells exposed to similar concentrations of different OPs in a number of studies (Harris et al. 2009a; Fowler et al. 2001; Sachana et al. 2003, 2005; Sidiropoulou et al. 2009). Since GAP-43 plays a key role during axon outgrowth, the current data together with previous findings strongly suggest that reduced level of GAP-43 might be a common molecular marker of sub-lethal neurite inhibitory effects of OPs.

The observed alterations in NFH phosphorylation were consistent with the possible disruption of cell signaling pathways. In the current study, it was important to relate these changes to the activation status of the MAP kinase ERK 1/2, since it known as a convergence point for cell signaling pathways involved in neuronal cell differentiation (Perron and Bixby 1999). This protein kinase is activated in N2a cells following induction of cell differentiation by serum withdrawal (Hargreaves et al. 2006) and such activation is required for the development of neurites (Singleton et al. 2000; Lopez-Maderuelo et al. 2001). Moreover, it is known to be important in the phosphorylation of NFH (Perron and Bixby 1999). The increase in reactivity of anti-pERK with no detectable changes in anti-total ERK antibody binding after 2 h exposure to both compounds suggested that OP treatment lead to increased activation of ERK, which could account for the changes in NFH phosphorylation at that time point. However, the lack of significant changes compared to the control after 4 and 8 h exposure suggested that the OP-induced activation of ERK 1/2 was short-lived.

On the other hand, the data obtained from the measurement of phosphatase activity compared to the controls were consistent with the possibility that increased phosphatase activity could account for the observed reduction in NFH phosphorylation at the later time point. Previously, it has been reported that protein phosphatase 2A from both rat spinal cord and rabbit skeletal muscle can reduce the phosphorylation of NFH following hyperphosphorylation by cyclin-dependent kinase-5 (cdk5) in neurodegenerative disease (Veeranna et al. 1995). In addition, reduced levels of protein phosphatases 2A and other phosphatases were found to be associated with enhanced NFH phosphorylation in protein aggregates found in Alzheimer's disease (Vogelsberg-Ragaglia et al. 2001) and amyotrophic lateral sclerosis brain (Kesavapany et al. 2007). Therefore, protein phosphatase 2A might be one potential NF-associated phosphatase involved in the reduced phosphorylation of NFH following 8 h exposure to both CPF and CPO. Further work to identify

specific phosphatases involved in the regulation of NFH phosphorylation in OP-treated cells would be worthwhile.

As previously discussed, the concentration of 3 µM CPF and CPO was chosen for most assays in the current study due to its ability to induce approximately 50 % reduction in both neurite outgrowth and in the number of pre-formed neurites in differentiating N2a cells. This concentration of CPF has clinical relevance to human developmental neurotoxicity, as median levels of 8.26 µg/ml (23.6 µM) are detectable in meconium samples of newborn children (Ostrea et al. 2002) and low micromolar levels of oxon metabolites are attainable in the developing human being (Flaskos 2012). Although oxon metabolites have higher water solubility than their parent compounds (Sogorb and Vilanova 2010), which would affect their ability to enter the fetus, the detection of significant cholinesterase inhibition in the mammalian fetus following in vivo exposure of pregnant animals to organophosphorothionate pesticides (Gupta 1995) suggests that fetal exposure to CPO can occur.

The fetus is thought to be exposed mainly to oxons formed in the maternal tissues; the main enzyme responsible for oxon formation in humans CYP2B6 (Foxenberg et al. 2007; Croom et al 2010) is present at relatively low levels in human placenta (Pelkonen et al 2006), suggesting that the placenta does not make a major contribution to oxon formation. However, although CYP2B6 is expressed at low levels in the human fetus compared to later stages of development (Croom et al. 2009), the fact that paraoxonase 1 (PON 1) levels are also relatively low at this stage (Costa et al 2005) could allow some oxon formation and/or accumulation in fetal tissue. Additionally, reduced levels of serum PON1 due to genetic polymorphisms in the PON1 gene would be associated with increased susceptibility to toxicity of the oxon metabolite (Costa et al. 2005). It could be argued that the concentrations of CPO used in the current study are unlikely to be attained *in vivo* and that the associated levels of AChE inhibition would be potentially lethal to the unborn child. On the other

hand, there are numerous clinical case studies of patients who, following accidental or intentional exposure, have survived very high levels of cholinesterase inhibition comparable to those observed in the current work, with the help of pharmacological intervention (e.g. by the administration of atropine and/or oximes). Survivors of CPF-induced acute cholinergic crisis (including both adults and children) can subsequently be affected by a delayed neuropathy involving dying back of axons in peripheral/central neurons (Clegg and Van Gemert 1999ab; Nand et al. 2007; Thivakaran et al. 2012). Furthermore, it has been shown that CPF administered at acute levels in animal models can lead to OPIDN (reviewed in Gupta, 2006).

It should be noted that the OP concentrations used in the current study are indicative of the maximum possible concentration of available OP. However, given that preliminary data (not shown) indicate an IC_{50} value for AChE following 4 h exposure of N2a cells to CPO of approximately 1 µM, compared to a value of 10 nM after 30 min exposure in rodent brain homogenates and 3 nM with immunoprecipitated AChE (Mortensen et al., 1998) it is possible that the indicative concentration was not reached in the cells, that the N2a cell line has limited uptake, the ability to detoxify CPO or that CPO rapidly loses activity in this cellular model. Further work to determine the actual concentration of OPs that enter the cells would be worthwhile.

From all of the results presented in this study, it can be concluded that the exposure of pre-differentiated N2a cells to non-cytotoxic concentrations of CPF and CPO results in rapid neurite retraction and major disruption of the neurofilament network. These effects are not dependent on the inhibition of AChE but are associated with an early transient increase in the phosphorylation of NFH by ERK 1/2, followed by protein phosphatase-mediated hypophosphorylation.

Acknowledgments:

We are grateful to Umm Al-Qura University in Saudi Arabia for funding this work.

Conflict of interest statement: The authors have no conflicts of interest to declare

References

Bhuyan BK, Loughman BE, Fraser TG, Day KJ (1976) Comparison of different methods of determining cell viability after exposure to cytotoxic compounds. Exp Cell Res 97: 274-280

Brown RE, Jarvis KL, Hyland KJ (1989) Protein measurement using bicinchoninic acid: elimination of interfering substances. Anal Biochem 180: 136–139

Campbell CG, Seidler FJ, Slotkin TA (1997) Chlorpyrifos interferes with cell development in rat brain regions. Brain Res Bull 43: 179-89

Clegg DJ, van Gemert M (1999a) Determination of the reference dose for chlorpyrifos: Proceedings of an expert panel. J Toxicol Environ Health-Part B-Crit Rev 2: 211-55

Clegg DJ, van Gemert M (1999b) Expert panel report on human studies of chlorpyrifos and/or other organophosphate exposures. J Toxicol Environ Health-Part B 2: 257-279

Costa L, Vitalone A, Cole TB, Furlong CE (2005) Modulation of paraoxonase (PON1) activity. Biochem Pharmacol 69: 541-50

Croom EL, Stevens JC, Hines RN, Wallace AD, Hodgson E (2009) Human hepatic CYP2B6 developmental expression: the impact of age and genotype. Biochem Pharmacol 78: 184-90

Croom EL, Wallace AD, Hodgson E (2010) Human variation in CYP specific chlorpyrifos metabolism. Toxicol 276: 184-91

Das KP, Barone S (1999) Neuronal differentiation in PC12 cells is inhibited by chlorpyrifos and its metabolites: Is acetylcholinesterase inhibition the site of action? Toxicol Appl Pharmacol 160: 217-30

Eaton DL, Daroff RB, Autrup H, Bridges J, Buffler P (2008) Review of the toxicology of chlorpyrifos with an emphasis on human exposure and neurodevelopment. Crit Rev Toxicol 38: 1-125

Ellman GL, Courtney KD, Andres V Jr, Featherstone RM (1961) A new and rapid colorimetric determination of acetylcholinesterase. Biochem Pharmacol 7:88–95

Flaskos J (2012) The developmental neurotoxicity of organophosphorus insecticides: A direct role for the oxon metabolites. Toxicol Lett 209: 86-93

Flaskos J, Harris W, Sachana M, Munoz D, Tack J, Hargreaves AJ (2007) The effects of diazinon and cypermethrin on the differentiation of neuronal and glial cell lines. Toxicol Appl Pharmacol 219: 172-80

Flaskos J, McLean WG, Fowler MJ, Hargreaves AJ (1998) Tricresyl phosphate inhibits the formation of axon-like processes and disrupts neurofilaments in cultured mouse N2a and rat PC12 cells. Neurosci Lett 242: 101-04

Flaskos J, Nikolaidis E, Harris W, Sachana M, Hargreaves AJ (2011) Effects of sub-lethal neurite outgrowth inhibitory concentrations of chlorpyrifos oxon on cytoskeletal proteins and acetylcholinesterase in differentiating N2a cells. Toxicol Appl Pharmacol 256: 330-36

Fowler MJ, Flaskos J, McLean WG, Hargreaves AJ (2001) Effects of neuropathic and non-neuropathic isomers of tricresyl phosphate and their microsomal activation on the production of axon-like processes by differentiating mouse N2a neuroblastoma cells. J Neurochem 76: 671-78

Foxenberg RJ, McGarrigle BP, Knaak JB, Kostyniak PJ, Olson JR (2007) Human hepatic cytochrome P450-specific metabolism of parathion and chlorpyrifos. Drug Metab Dispos 35: 189-93

Gupta RC (1995) Environmental agents and placental toxicity: anticholinesterases and other agents. In: Sastry BVR (ed.). Placental toxicity. CRC Press, Boca Raton, pp 257-78.

Hargreaves AJ, Fowler MJ, Sachana M, Flaskos J, Bountouri M (2006) Inhibition of neurite outgrowth in differentiating mouse N2a neuroblastoma cells by phenyl saligenin phosphate: Effects on MAP kinase (ERK 1/2)

activation, neurofilament heavy chain phosphorylation and neuropathy target esterase activity. Biochem Pharmacol 71: 1240-47

Harris W, Munoz D, Bonner PLR, Hargreaves AJ (2009a) Effects of phenyl saligenin phosphate on cell viability and transglutaminase activity in N2a neuroblastoma and HepG2 hepatoma cell lines. Toxicol in Vitro 23: 1559-63

Harris W, Sachana M, Flaskos J, Hargreaves AJ (2009b). Proteomic analysis of differentiating neuroblastoma cells treated with sub-lethal neurite inhibitory concentrations of diazinon: Identification of novel biomarkers of effect. Toxicol Appl Pharmacol 240: 159-65

Howard AS, Bucelli R, Jett DA, Bruun D, Yang DR, Lein PJ (2005) Chlorpyrifos exerts opposing effects on axonal and dendritic growth in primary neuronal cultures. Toxicol Appl Pharmacol 207: 112-24

Keilbaugh SA, Prusoff WH, Simpson MV (1991) The PC12 cell as a model for studies of the mechanism of induction of peripheral neuropathy by anti-HIV-1 dideoxynucleoside analogs. Biochem Pharmacol 42: R5-R8

Kesavapany S, Patel V, Zheng YL, Pareek TK, Bjelogrlic M, Albers W, Amin N, Jaffe H, Gutkind JS, Strong MJ, Grant P, Pant HC (2007) Inhibition of Pin1 reduces glutamate-induced perikaryal accumulation of phosphorylated neurofilament-H in neurons. Mol Biol Cell 18(9): 3645–3655

Laemmli UK (1970) Cleavage of structural proteins during assembly of head of bacteriophage-t4. Nature 227: 680

Larkin DJ, Tjeerdema RS (2000) Fate and effects of diazinon. Rev Env Contam Toxicol 166: 49-82

Lee VMY, Otvos L, Carden MJ, Hollosi M, Dietzschold B, Lazzarini RA (1988) Identification of the major multiphosphorylation site in mammalian neurofilaments. Proc Natl Acad Sci U.S.A 85: 1998-2002

Lock EA, Johnson MK (1990) Delayed neuropathy and acute toxicity studies with pirimiphos-methyl in the hen. J Appl Toxicol 10: 17-21

Lopez-Maderuelo MD, Fernandez-Renart M, Moratilla C, Renart J (2001) Opposite effects of the Hsp90 inhibitor Geldanamycin: induction of apoptosis in PC12, and differentiation in N2A cells. FEBS Lett 490: 23-27

Lotti M (2005) Organophosphate induced delayed polyneuropathy (OPIDP): Features and mechanisms. Toxicology 213: 210-11

Lotti M, Moretto A (2005) Organophosphate-induced delayed polyneuropathy. Toxicol Rev 24: 37-49

Mortensen SR, Brimijoin S, Hooper MJ, Padilla S (1998) Comparison of the in vitro sensitivity of rat acetylcholinesterase to chlorpyrifos-oxon: What do tissue IC50 values represent? Toxicol Appl Pharmacol 148: 46-49.

Mosmann T (1983) Rapid colorimetric assay for cellular growth and survival - application to proliferation and cyto-toxicity assays. J Immunol Meth 65: 55-63

Nand N, Aggarwal HK, Bharti K, Chakrabarti D (2007) Organophosphate induced delayed neuropathy. JAPI 55: 72-73

Ostrea EM, Morales V, Ngoumgna E, Prescilla R, Tan E, Hernandez E, Ramirez GB, Cifra HL, Manlapaz ML (2002) Prevalence of fetal exposure to environmental toxins as determined by meconium analysis. Neurotoxicology 23:329-339

Pelkonen O, Vahakangas K, Gupta RC (2006) Placental toxicity of organophosphate and carbamate pesticides. In: Gupta RC (ed.) Toxicology of Organophosphate and Carbamate Compounds. Elsevier Academic Press, Burlington, pp. 463-79

Perron JC, Bixby JL (1999) Distinct neurite outgrowth signaling pathways converge on ERK activation. Mol Cell Neurosci 13: 362-78

Richardson RJ (1995) Assessment of the neurotoxic potential of chlorpyrifos relative to other organophosphorus compounds - a critical-review of the literature. J Toxicol Environ Heal 44: 135-65

Sachana M, Flaskos J, Alexaki E, Glynn P, Hargreaves AJ (2001) The toxicity of chlorpyrifos towards differentiating mouse N2a neuroblastoma cells. Toxicol In Vitro 15: 369-72

Sachana M, Flaskos J, Alexaki E, Hargreaves AJ (2003) Inhibition of neurite outgrowth in N2a cells by leptophos and carbaryl: effects on neurofilament heavy chain, GAP-43 and HSP-70. Toxicol In Vitro 17: 115-20

Sachana M, Flaskos J, Hargreaves AJ (2005) Effects of chlorpyrifos and chlorpyrifos-methyl on the outgrowth of axon-like processes, tubulin, and GAP-43 in N2a cells. Toxicol Mech Meth 15: 405-10

Sidiropoulou E, Sachana M, Flaskos J, Harris W, Hargreaves AJ, Woldehiwet Z (2009) Diazinon oxon affects the differentiation of mouse N2a neuroblastoma cells. Arch Toxicol 83: 373-380

Singleton DW, Lu CL, Colella R, Roisen FJ (2000) Promotion of neurite outgrowth by protein kinase inhibitors and ganglioside GM1 in neuroblastoma cells involves MAP kinase ERK1/2. Inter J Develop Neurosci 18: 797-805

Skene JHP (1989) Axonal growth-associated proteins. Ann Rev Neurosci 12: 127-56

Slotkin TA, Levin ED, Seidler FJ (2006) Comparative developmental neurotoxicity of organophosphate insecticides: Effects on brain development are separable from systemic toxicity. Environ Health Perspect 114: 746-51

Sogorb MA, Vilanova E (2010) Detoxification of anticholinesterase pesticides. In: Satoh T, Gupta RC (eds) Anticholinesterase pesticides: Metabolism, neurotoxicity and epidemiology. Wiley, Hoboken NJ, pp 121-32

Steevens JA, Benson WH (1999) Toxicological interactions of chlorpyrifos and methyl mercury in the amphipod, Hyalella azteca. Toxicol Sci 52: 168-77

Thivakaran T, Gamage R, Gunarathne KS, Gooneratne IK (2012) Chlorpyrifos-induced delayed myelopathy and pure motor neuropathy: a case report. Neurologist 18: 226-228

Towbin H, Staehelin T, Gordon J (1979) Electrophoretic transfer of proteins from polyacrylamide gels to nitrocellulose sheets - procedure and some applications. Proc Natl Acad Sci *U.S.A* 76: 4350-54

Veeranna S, Shetty KT, Link WT, Jaffe H, Wang J, Pant HC (1995) Neuronal cyclin-dependent kinase-5 phosphorylation sites in neurofilament protein (NF-H) are dephosphorylated by protein phosphatase 2A. J Neurochem 64:2681–2690

Veeranna NDA, Ahn NG, Jaffe H, Winters CA, Grant P, Pant HC (1998) Mitogen-activated protein kinases (ERK1/2) phosphorylate Lys-Ser-Pro (KSP) repeats in neurofilament proteins NF-H and NF-M. J Neurosci 18: 4008-21

Vogelsberg-Ragaglia V, Schuck T, Trojanowski JQ, Lee VM (2001) PP2A mRNA expression is quantitatively decreased in Alzheimer's disease hippocampus. Exp Neurol 168(2): 402–412

Williamson TL, Marszalek JR, Vechio JD, Bruijn LI, Lee MK, Xu Z, Brown RH, Cleveland DW (1996) Neurofilaments, radial growth of axons, and mechanisms of motor neuron disease. Cold Spring Harbor Symp Quant Biol 61: 709–723